HAL open science

Fatigue damage mechanisms in steel cable under bending loading

Matthieu Bonneric, Véronique Aubin, Damien Durville

To cite this version:

Matthieu Bonneric, Véronique Aubin, Damien Durville. Fatigue damage mechanisms in steel cable under bending loading. Engineering Failure Analysis, 2019, 106, pp.104184 -. 10.1016/j.engfailanal.2019.104184 . hal-03489021

HAL Id: hal-03489021

https://hal.science/hal-03489021v1

Submitted on 20 Jul 2022

HAL is a multi-disciplinary open access archive for the deposit and dissemination of scientific research documents, whether they are published or not. The documents may come from teaching and research institutions in France or abroad, or from public or private research centers.

L'archive ouverte pluridisciplinaire **HAL**, est destinée au dépôt et à la diffusion de documents scientifiques de niveau recherche, publiés ou non, émanant des établissements d'enseignement et de recherche français ou étrangers, des laboratoires publics ou privés.

Distributed under a Creative Commons Attribution - NonCommercial 4.0 International License

Version of Record: https://www.sciencedirect.com/science/article/pii/S1350630719304753
Manuscript_9a8c0b589b8313c711011d27ebcfd446

Fatigue damage mechanisms in steel cable under bending loading

Matthieu Bonneric[a], Véronique Aubin[a,*], Damien Durville[a]

[a] *MSSMat Laboratory, CentraleSupélec, CNRS UMR8579, Université Paris-Saclay*

Abstract

Steel cables can be employed as reinforcements in complex structures. During their use in service, they might be subjected to cyclic loadings leading to fatigue damage. This work deals with the fatigue damage evolution in steel cables used in tires, when subjected to cyclic bending loadings corresponding to some extreme in-service uses of tires. The studied cables are embedded in an elastomer matrix, as required for this application. First, a specific experimental device has been developed to test elastomer-steel cable composite specimens. In order to study damage mechanisms, specimens were observed in a bent position using X-ray tomography after fatigue testing. Crack distribution was analyzed for two distinct loading amplitudes. SEM observations of the crack initiation zones were also made to complete the analysis. Secondly, finite-element analysis was carried out. The bent cable and its matrix were simulated both with and without broken wires, in order to evaluate the impact of the first breakage on the stress distribution within the cable. Eventually, the combination of observations and simulations allowed to propose two damage mechanisms, depending on the loading severity.

Keywords:

steel cable, bending fatigue, damage mechanisms, finite element

1. Introduction

Steel cables can be employed for various applications (elevator ropes, bridges suspensions, tire reinforcements, etc...). During their use in service, cables are usually subjected to a combination of cyclic tension and bending leading to fatigue damage. Therefore, the evaluation of their fatigue behavior is an important

*MSSMat Laboratory, CentraleSupélec, CNRS UMR8579, Université Paris-Saclay
Email address: veronique.aubin@centralesupelec.fr, Tel: +33175316520 (Véronique Aubin)

© 2019 published by Elsevier. This manuscript is made available under the CC BY NC user license
https://creativecommons.org/licenses/by-nc/4.0/

issue to guarantee structures' integrity. Besides, the understanding of damage mechanisms at the cable scale is also an important matter, not only to propose relevant prediction tools, but also to improve cable design with respect to fatigue performance.

Most of the works that can be found in the literature about the fatigue of cable focused on tension-tension loadings or cyclic bending with constant pre-tension. Suh et al exhibited the significant influence of both stress amplitude and mean stress on the fatigue life of multi-strand cables subjected to axial loading [1]. Kim et al observed the evolution of broken wires in a multi-strand cable subjected to a cyclic bending and a constant pre-tension, and investigated the impact of the cyclic loading on the residual tensile strength [2]. Zhang et al studied the fatigue damage of a multi-strand cable subjected to a cyclic bending loading applied through pulleys and constant pre-tension [3]. In particular, they observed the spatial distribution of wire breaks along cable length, and its evolution with the number of applied cycles. In a more recent study, Zhang et al also investigated the influence of pre-broken wires on the fatigue damage mechanisms [4]. The presence of pre-broken wires is found to be responsible for a significant decrease in the fatigue life, with fatigue damage concentrated on the surface of the pre-broken wires' lay length and adjacent lay lengths. The authors attributed this localized damage to the severe wear resulting from the change of the stress state of the inner strand at the level of pre-broken wires.

In a more general way, all these works report that fatigue damage results either from fretting-fatigue or wear, in accordance with earlier studies that had already shown the importance of inter-wire contact phenomena on the fatigue damage mechanisms of cables [5, 6]. Many efforts have thus been made to characterize fretting-fatigue phenomenon between wires [7–10] and to predict the resulting fatigue life of cables [11, 12].

Some authors also reported that when the contribution of the axial load is insignificant, the failure of cable results from pure fatigue damage instead of fretting-fatigue or wear-induced damage [2], [10]. However, to the best of the authors' knowledge, there is no existing study about the fatigue damage of a cable subjected to cyclic bending without the presence of an axial load that would enhance fretting-fatigue, likely due to the limited number of applications concerned in this situation. Yet, when steel cables are used as reinforcements

in tires, they might be subjected to such a loading for some specific in-service uses, when tires are running flat.

This work aims to tackle this issue, and deals with the fatigue damage mechanisms in a high strength steel monostrand cable subjected to a high cyclic bending loading. As required for tire applications, cables are embedded in an elastomer matrix, and a specific experimental device has been developed to perform bending fatigue on composite elastomer-steel cables specimens. In order to study the influence of the loading amplitude on the damage mechanisms, X-ray tomography was used to observe the spatial distribution of cracks, as well as finite-element analysis.

2. Experimental approach

2.1. Materials and specimens

The cable studied in this work has 19 wires wounded on 3 layers, as shown in figure 1. The layers #2 and #3 are made of wires of 175 µm diameter (Wire 1). They are winded with a pitch length of 10 mm around the layer #1, which is a straight wire of 200 µm diameter (Wire 2). All the wires are made of pearlitic steel, and coated with a thin layer of brass. They are obtained by a cold drawing process allowing to reach high mechanical properties ($\sigma_u > 2500$ MPa) and very thin diameters.

The specimens used for fatigue testing are parallel steel cables immersed in an elastomer layer of 3 mm thickness (figure 2). These specimens are obtained by calendering before vulcanizing the elastomer matrix, with the cables in the middle of the specimen thickness. The presence of the elastomer impacts on wire

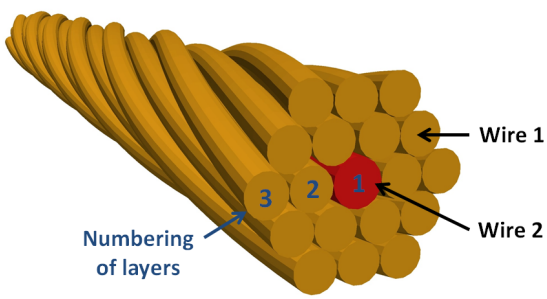

Figure 1: Schematic representation of the geometry of the 19-wire cable studied

Figure 2: Transverse cut of a composite specimen

kinematics, and is necessary to apply bending loadings that are representative of tire applications. Indeed, the presence of the elastomer around the cable tends to limit any cable opening when the bending loading is applied. Besides, the wire brass coating reacts with the elastomer during vulcanization, resulting in an adhesive bonding between the wires from layer #3 (the only ones in contact with the matrix), and the matrix.

2.2. Fatigue test procedure

A specific device was developed in order to apply a high cyclic bending loading to the composite specimens that have been previously described. This experimental set-up is shown in figure 3. The composite specimen is bent between two rigid planes. One of the planes, whose position is adjusted within a few millimeter range prior to fatigue testing, is fixed, whereas the second plane is subjected to a cyclic translation motion by

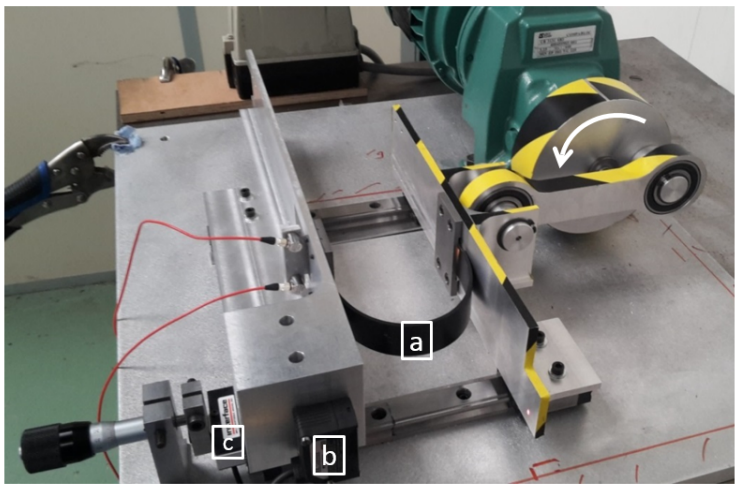

Figure 3: View of experimental device used to perform bending fatigue tests. a) Bent specimen b) Position sensor c) Load cell

means of a crank rod system. The set-up makes it possible to apply a 86 mm displacement to the second plane at a 7.6 Hz frequency, which was not possible with a hydraulic machine.

The bending loading applied to the cables can be defined by the radius R of the quasi-circle formed by the median fiber of the bent specimen, where cables are located. This quantity can be calculated using the following expression:

$$R = \frac{1}{2}(d - t) \tag{1}$$

where d is the distance between the two planes and t the specimen thickness. The minimum and maximum values R_{min} and R_{max} reached by this parameter over a cycle are respectively about 7 mm and 50 mm, the exact values depending on the position of the fixed plane. Indeed, as mentioned before, the position of the fixed plane can be adjusted within a 5 millimeter range prior to fatigue testing, resulting in modifications of both R_{min} and R_{max}. It was assumed that modifying R_{max} within a few millimeter range has no significant impact on the stress distribution in wires, which are then subjected to very little stress. Therefore, in the present study, R_{max} was considered as constant, and the severity of the bending loading was entirely controlled by the minimum radius R_{min}, designated as R_c in what follows.

During the test, the minimum distance between the two planes over a cycle is monitored with a position sensor. Considering both the uncertainty of the position of the cables in the specimen thickness and the sensor precision, the uncertainty associated with the estimation of the radius R_c is less than 0.1 mm. A load cell of 450 N capacity is also employed to measure the force applied to the bent specimen with a 0.2 N precision. This measurement allows to detect cable damage, wire breakages leading to a decrease of the bending stiffness of the specimen, and therefore to a drop in the load measurement.

In order to validate this experimental device, fatigue tests have been performed for various loading amplitudes. Figure 4 provides the evolution of the number of cycles N_r for which the failure of the specimen is reached, as a function of the minimum radius R_c. Even if the fatigue performance appears to be very sensitive to the radius R_c, the good correlation between this parameter and the fatigue life demonstrates a satisfying control of the applied loading. Besides, it can be noted that the present set-up makes it possible

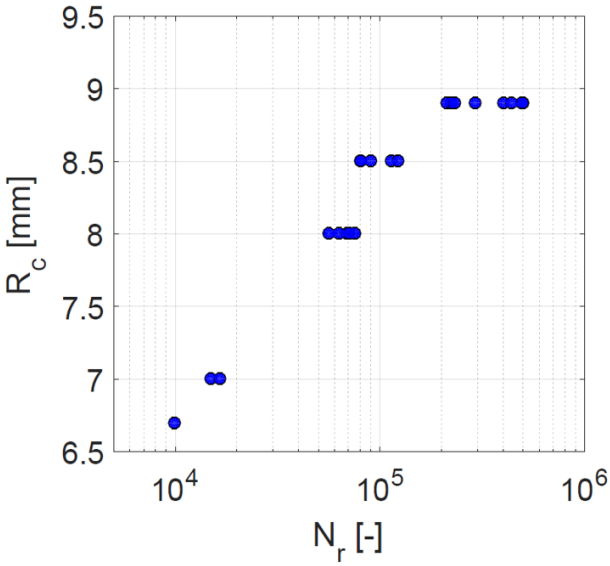

Figure 4: Evolution of the fatigue life with respect to the applied loading characterized by the radius R_c

to investigate damage mechanisms for a wide range of fatigue lives, from 10^4 cycles to 10^6 cycles.

In the present study, 2 particular loading amplitudes were considered. The first one corresponds to $R_c = 7\,\text{mm}$ and leads to fatigue lives of about 10^4 cycles, whereas the second one corresponds to $R_c = 8.5\,\text{mm}$, for which fatigue lives are about 10^5 cycles. The first loading leading to early fatigue damage, it is referred as severe bending in what follows. In opposition, the second one is referred as moderate bending.

In order to study damage mechanisms, fatigue tests were conducted and interrupted at different stages of damage on specimens containing only one cable. The cables were then observed using X-ray tomography after fatigue testing, as described in the next section. SEM observations of the fracture surfaces of wires were also carried out after removing the wire-matrix adhesive bonding by electrolysis, and extracting the cable from the matrix.

2.3. Characterization of crack distribution

In order to determine the spatial crack distribution resulting from fatigue testing, X-ray tomography was employed. The cable to be observed is inserted in a tube, and the area of interest, prior subjected to the minimum radius R_c during the test, is maintained in a bent position using 3 screws as shown in figure 5. The bending is applied in the same direction as in the test, but with a greater radius of curvature so that

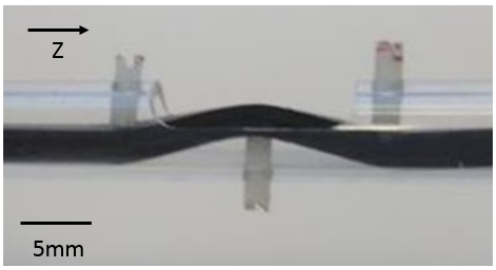

Figure 5: 3-point bending of a specimen for X-ray tomography observations

no further damage is induced. By doing so, the cracks are opened in order to facilitate their detection. It can be noted that the cable was not extracted from the matrix. Indeed, keeping the matrix allows to preserve the exact orientation of the cable as it was during the test, with the aim of comparing the damage observations with the stress distribution in wires simulated by finite elements.

The spatial resolution obtained for tomography measurement was between 5 mm and 6 mm. The wire breaks and the fatigue cracks close to final failure (cracks whose depth was greater than 50 µm) were identified for each sample. They are both designated as cracks in what follows. It is worth mentioning that the number of cracks detected in each sample was very well correlated to the load drop for which the test was interrupted (figure 6). This correlation demonstrates the relevance of using load measurements to detect cable damage. In order to analyze the spatial distribution of damage, the crack distribution along the Z axis indicated in

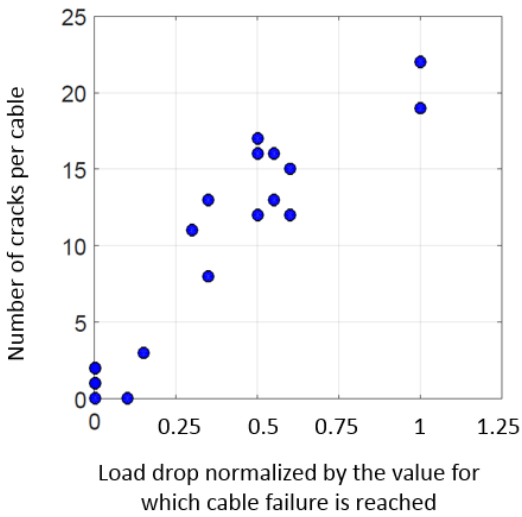

Figure 6: Evolution of the number of the detected cracks in specimens containing one cable with respect to load drop

figure 5 was considered. The latter provides a description of damage distribution along cable direction. In addition, a schematic view of a cable transverse section on which are projected the transverse position of the detected cracks was also made up for each sample.

3. Results

3.1. SEM observations

Figure 7 provides SEM observations of 2 damaged wires extracted from cables tested with a severe bending loading. No contact scars were observed at the level of the crack initiation sites, indicating that the damage in wires does not result from wear or fretting. As also reported in [2], [10], these observations suggest that inter-wire contact phenomena do not play a significant role in fatigue damage mechanisms when the tension applied to cable, which is zero in the present study, is low. SEM observations also showed that fatigue cracks initiate and remain mostly contained in wire transverse sections. It can therefore be assumed that fatigue damage is driven by the longitudinal stress in wires.

However, crack bifurcation in the longitudinal direction past the first stages of propagation was sometimes observed (figure 7a). This phenomenon was already mentioned in a past study dealing with the fatigue failure of cables, and was associated with a localized bending of wires [6]. Besides, it is well known that the drawing

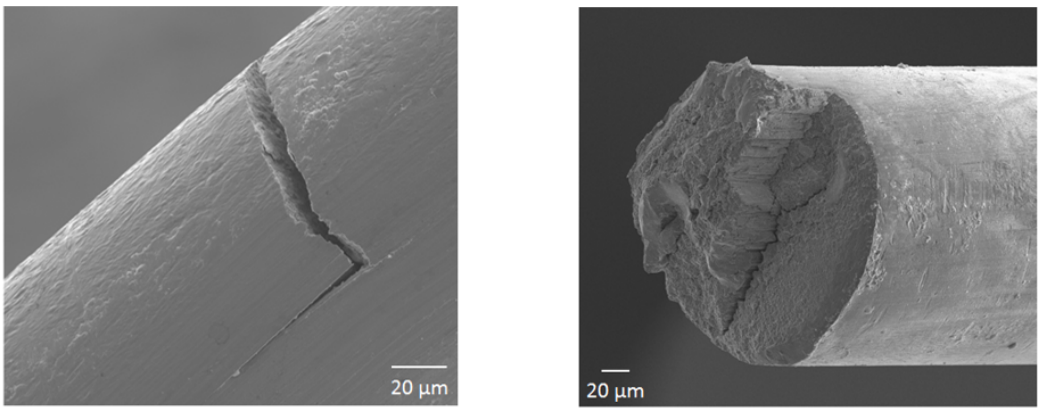

(a) (b)

Figure 7: SEM observations of damaged wires after bending fatigue testing

process tends to align the pearlitic lamellae in steel wires [13], resulting in a failure anisotropy of the material [14]. It was therefore not surprising to observe such changes in the crack paths in the present work.

3.2. Observations of the spatial crack distribution

Figure 8 shows 2 longitudinal slices from tomography measurements on 2 cables, exhibiting the typical damage distributions for the 2 loading amplitudes $R_c = 7\,\text{mm}$ and $R_c = 8.5\,\text{mm}$. The 2 cables analyzed have approximately the same number of cracks, with 16 cracks in the cable subjected to severe bending and 19 cracks in the one subjected to moderate bending. It can be observed in figure 8a that cracks seem to be uniformly distributed within a few millimeter range along the cable direction when severe bending is applied. Crack distribution appears to be different for moderate bending, for which cracks are localized in the vicinity of one cable section in the bent area (figure 8b). In order to support these visual observations, the crack distribution along the Z axis has been calculated for 4 cables for both severe and moderate bending. Figure 9 provides the mean distributions of the fatigue cracks so obtained for of each the studied loadings. The two distributions are significantly different from each other, consistently with previous observations. For severe bending, crack development is possible within a 8 mm range, resulting in a wider distribution

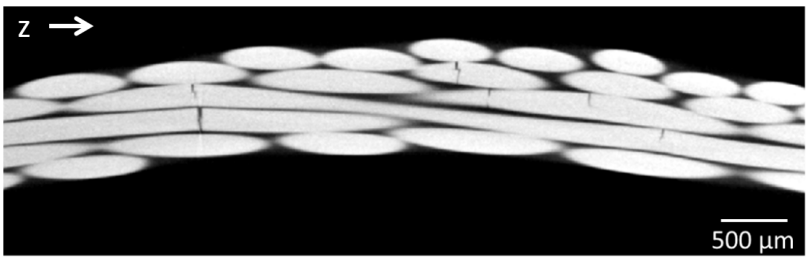

(a) Typical crack distribution for severe bending ($R_c = 7\,\text{mm}$)

(b) Typical crack distribution for moderate bending ($R_c = 8.5\,\text{mm}$)

Figure 8: X-ray tomography observations after bending fatigue tests

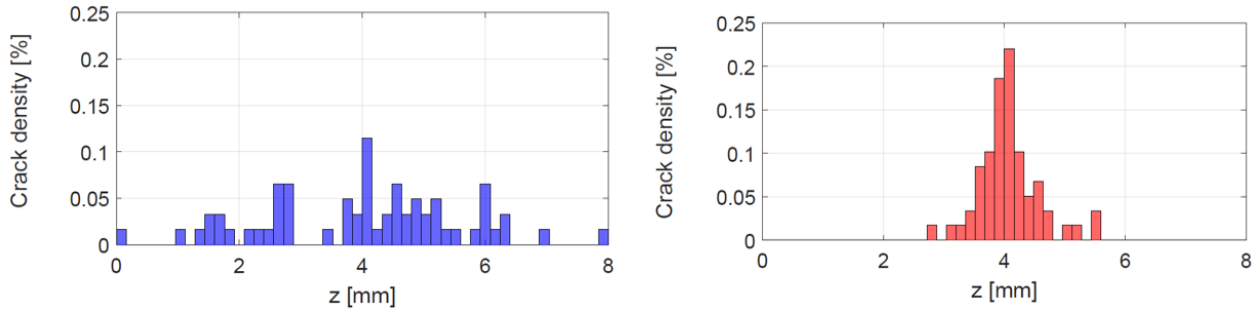

(a) Severe bending ($R_c = 7\,\text{mm}$)

(b) Moderate bending ($R_c = 8.5\,\text{mm}$)

Figure 9: Mean distribution of fatigue cracks along Z-axis from 4 different specimens

than for moderate bending, for which cracks are localized near a single cable section, within a 3 mm range.

The spatial distribution of fatigue cracks within cable transverse section was also analyzed. Figure 10 shows the obtained results for 4 cables, corresponding either to severe or moderate bending. For each cable, the regions where cracks have been detected are colored, differentiating areas in the top of the cable with respect to the bending loading (in red), areas in the bottom of cable (in blue), and areas at the level of the median fiber of the cable (in green). The number of detected cracks detected is also indicated. It should be mentioned that when several cracks are in the same place on this view, they are not necessarily associated to the same wire, wires of layers #2 and #3 being helically wound. One can then note that severe and moderate bending do not lead to the same crack distribution. For severe bending, at least 65 % of the cracks are at the level of the median fiber or at the bottom of cable, whereas 45 % to 60 % of the cracks are on the top of cable for moderate bending.

Thus, all the results show that severe bending does not lead to the same distribution of fatigue cracks that for moderate bending. It can therefore be assumed that the damage mechanisms leading to cable failure are not the same for the 2 loadings. This issue is investigated in the next section by carrying finite-element analysis.

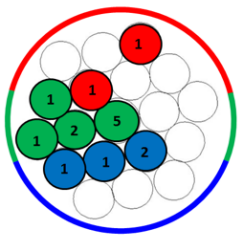

(a) Cable subjected to severe bending - 15 cracks

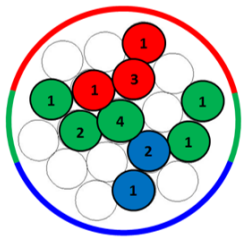

(b) Cable subjected to severe bending - 17 cracks

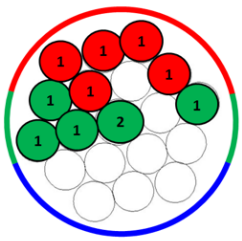

(c) Cable subjected to moderate bending - 11 cracks

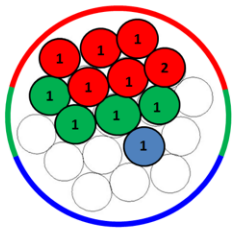

(d) Cable subjected to moderate bending - 12 cracks

Figure 10: Projections of the fatigue cracks in a transverse cut of the cable. The red color indicates points above the median fiber (top of the bent cable); the blue color indicates the points below the median fiber (bottom of the bent cable); the green color the points at the level of the median fiber.

4. Finite-element analysis and discussion

4.1. Analysis of the stress distribution in wires

The cyclic bending of a cable has been simulated using finite-element. In order to be consistent with the loading applied during fatigue testing, the elastomer matrix surrounding the cable has been accounted for, and 2 rigid planes have been used to enforce boundary conditions as shown in figure 11. A complete description of the model, its parameterization, and its validation against experimental measurements can be found elsewhere [15]. Though, it is to be noted that beam elements were used to model the wires, and that the elastoplastic behavior of wires has been considered.

Figure 12a shows the typical distribution of the longitudinal stresses in the middle of the specimen when the cable is highly bent. One can see that every wire is subjected to a significant bending, and that the stress varies from several thousands of MPa within wire section. The bending of wires being predominant,

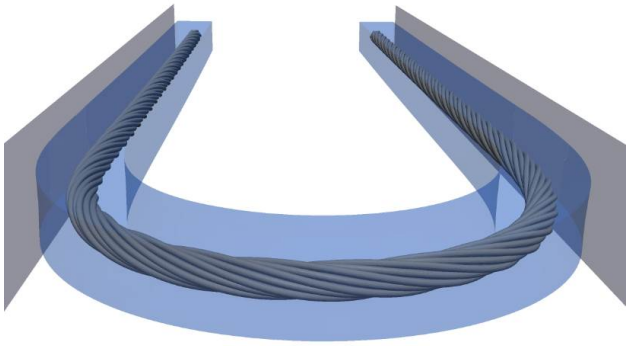

Figure 11: View of the simulated bent specimen

the following analysis only focuses on the longitudinal stresses in wires. In particular, attention is paid to the maximum longitudinal stresses at the surface of wires. In order to dispose of an appropriate scale to compare the maximum stresses from different wires, the value of the maximum stress in each wire section is attributed to the whole wire section when displaying the results. This results in a single color for each wire section on the viewing, as shown in figure 12b.

Cycles were performed between the radius's R_{max} and R_{min} for both severe and moderate bending. The distributions of stress amplitudes $\Delta\sigma$ and load ratios were computed for the bent area. Distributions were stabilized after 2 cycles. It was found that the load ratio values are contained within a narrow window between 0.05 and 0.2. Thus, in order to facilitate the interpretation of the numerical results with respect to fatigue damage mechanisms, all the stress amplitudes analyzed in what follows were normalized with respect

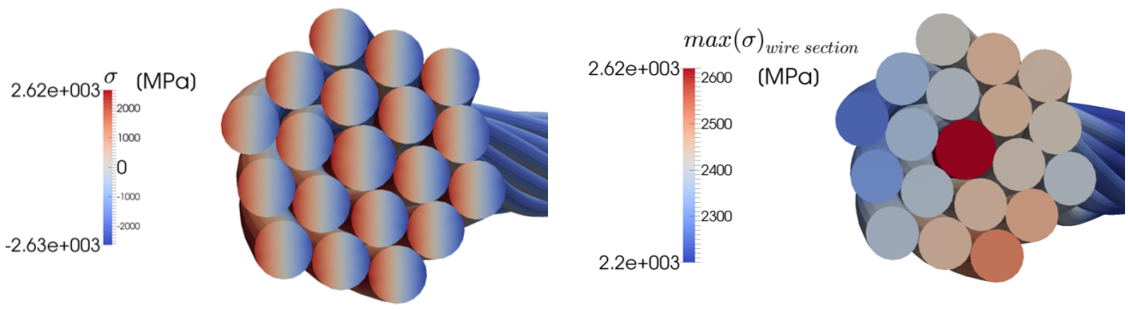

(a) Display of the longitudinal stress

(b) Display of the maximum longitudinal stress for each wire section

Figure 12: Visualization of the spatial distribution of the longitudinal stresses within a transverse section of cable in the middle of the bent area

to the fatigue resistance of wires in tension $\Delta\sigma_d$, assessed at 10^5 cycles for a load ratio of 0.1.

Figure 13 presents the stress amplitudes in the 3 layers of the cable for both severe and moderate bendings, and highlights the areas stressed above the fatigue limit. In addition, figure 14 shows how the stress is distributed in the cable section located in the middle of the bent area. For severe bending, it is observed that all the wires are stressed above the fatigue limit in the bent area. These results are consistent with previous observations for severe bending, where cracks were found to be distributed within a wide portion of the bent area. Moreover, the stress distribution shown in figure 14a is also in good correlation with the distribution of cracks (figures 10a and 10b). Indeed, most of the cracks are at the level of the median fiber and the bottom of the cable, which coincides with the higher stresses. A significant difference in stress between the core wire and other wires can also be pointed out. The latter is mainly due to the fact that the

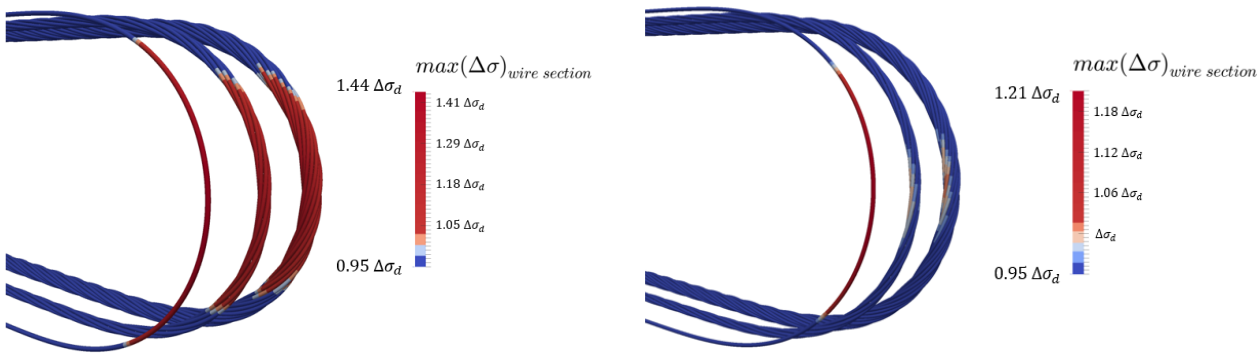

(a) $R_c = 7\,\text{mm}$ (b) $R_c = 8.5\,\text{mm}$

Figure 13: Exploded view of the 3 layers of the bent cable - Display of the maximum stress in each wire section

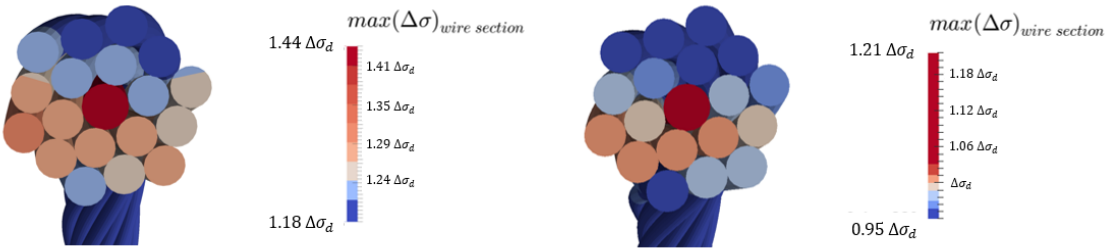

(a) $R_c = 7\,\text{mm}$ (b) $R_c = 8.5\,\text{mm}$

Figure 14: Spatial stress distribution within a transverse section of cable in the middle of the bent area - Display of the maximum stress in each wire section

core wire diameter is 14 % larger than for other wires, leading to higher stresses under bending loading. This is also consistent with the previous observations of cables prior subjected to the severe bending. The latter exhibited multiple cracks in the core wire that were not observed for the other wires (figures 10a and 10b), reflecting then the difference in stress between the core wire and other wires. The very good agreement between damage observations and simulation of the bending of an undamaged cable makes it possible to conclude about the mechanism leading to cable failure for the case of a severe bending. Thus, when the bending loading is such as a large part of the bent area is stressed above the wire fatigue resistance, many cracks can initiate all along the bent area, independently from each other. The propagation of these cracks until the wires break is then responsible for cable failure.

For moderate bending, only the core wire is highly stressed above the fatigue limit all along the bent area. The stress in other wires from layers #2 and #3 barely exceeds the fatigue limit, and only for some specific regions in middle of the bent area (figure 13b). However, as opposed to severe bending, the distribution of the stresses shown in 14b is not consistent with damage distribution, since a significant part of the cracks are on the top of the cable while this area is stressed well below the fatigue limit. Therefore, it can be assumed that crack initiation on the top of the cable only becomes possible once the first wires are broken, after a redistribution of the stresses. In order to check on this assumption, a simulation of the bending of a cable containing a broken wire have been carried out.

4.2. Influence of the first wire break on the stress distribution

Previous analysis showed that the core wire is highly stressed all over the bent area for moderate bending, whereas the stress in other wires barely exceeds the fatigue limit, and only in some specific regions. Based on simulation results, it can therefore be assumed that the first wire that is likely to break in case of moderate bending is the core wire. Besides, 2 additional fatigue tests interrupted at an early stage of damage, before any drop in the load measurement, have been performed. X-ray tomography observations of the cables then confirmed that the first wire to break is the core wire. In order to account for the first wire break in the simulation, the stiffness of a beam element of the core wire located in the middle of the bent area was set to zero. The break was introduced in the bent position after 2 cycles corresponding to moderate bending,

and an additional cycle was performed with the broken wire before analysing stress distribution. Although this modelling of the wire break does not account for the separation of the two ends of the broken wires, it is assumed that it provides an acceptable description of the broken wire within the bent cable, the presence of the neighboring undamaged wires limiting the separation of the 2 broken ends. Figure 15 shows how the trajectory taken by the core wire within the bent cable is affected by the break. Although the curvature is lower on both side of the break, it is locally increased at the level of the break. This local increase in cable curvature results in a significant increase in the stress at the level of the cable section corresponding to the break. This can be observed in figure 16 that provides 3D views of the stress distributions in the cable section in the middle of the bent area obtained respectively with and without the wire break, for the case of moderate bending. One can note that the wires on the top of the cables are stressed above the fatigue limit, confirming that crack initiation is possible once the core wire is broken. Besides, it can be seen in figure 16b that this increase in stress only concerns the damaged cable section, and that the stress in wires is much lower apart from this section. This is consistent with the distribution of cracks observed with X-ray tomography for moderate bending, for which cracks were localized at the level of a single cable section.

Thus, the previous analysis of the redistribution of the stresses once a wire is broken makes it possible to clarify the damage mechanism leading to cable failure for the case of moderate bending. In a general way, when a cable is subjected to a bending such as only a few wires are stressed above the fatigue limit, only

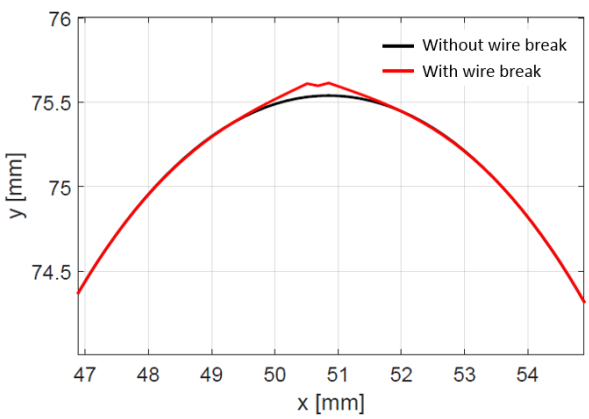

Figure 15: Modification of the trajectory taken by the core wire after its break for the case of moderate bending

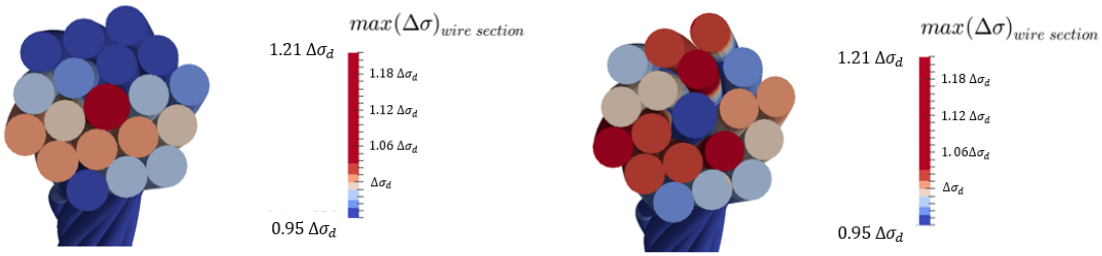

(a) Without the core wire broken

(b) With the core wire broken

Figure 16: Stress distribution within a transverse section of cable in the middle of the bent area - Influence of the first breakage for $R_c = 8.5\,\mathrm{mm}$

a few cracks can initiate in a first place. In a second place, the first wire breaks lead to a local increase of the curvature at the level of the damaged sections. This results in a significant increase of the stresses at the level of these sections, responsible for the initiation and the propagation of new fatigue cracks, leading eventually to cable failure.

5. Conclusions

The results of this work can be summarized as follows:

1. A specific experimental device has been developed to subject steel cables to high cyclic bending loadings, with the aim of reproducing some specific loadings that could be encountered for tire applications.
2. SEM observations of the fracture surfaces revealed that inter-wire contact phenomena do not induce wear or fretting-fatigue damage for these bending loadings. Instead, cable failure results from the pure fatigue damage of the wires, that are individually subjected to a high bending.
3. For the cable considered in this study, two damage mechanisms leading to cable failure were evidenced, combining X-ray tomography observations and finite-element simulations. When a severe bending is applied, such as a large part of the bent area is stressed above the wire fatigue resistance, many cracks can initiate all along the bent area, independently from each other. The propagation of these cracks until the wire breaks is then responsible for the cable failure. Cracks are then distributed within a wide portion of the bent area. When a moderate bending is applied, such as only the core wire is stressed

above the fatigue limit, only a few cracks can initiate in a first place, at the level of the core wire. Once the core wire is broken, the cable curvature locally increases, resulting in a significant increase of the stresses at the level of the damaged section. New fatigue cracks can then initiate and propagate, leading cable to failure. For such a case, as opposed to severe bending, the cracks are localized in the vicinity of the cable section where the first crack occurred.

Acknowledgments

This work has been financially supported by the French "Agence Nationale de la Recherche," through the "Investissements d'avenir" program (ANR-10- EQPX-37 MATMECA Grant), and by the French tyre manufacturer MICHELIN (Grant number: A10-5127).

References

[1] J. Suh, S. Chang, Experimental study on fatigue behaviour of wire ropes, International Journal of Fatigue 22 (2000) 339–347.

[2] S. Kim, R. Bae, J. Kwon, Bending fatigue characteristics of wire rope, Journal of Mechanical Science and Technology 26 (7) (2012) 2107–2110. doi:10.1007/s12206-012-0524-2.

[3] D. Zhang, K. Chen, X. Jia, D. Wang, S. Wang, Y. Luo, S. Ge, Bending fatigue behaviour of bearing ropes working around pulleys of different materials, Engineering Failure Analysis 33 (2013) 37–47. doi:10.1016/j.engfailanal.2013.04.018.

[4] D. Zhang, C. Feng, K. Chen, D. Wang, X. Ni, Effect of broken wire on bending fatigue characteristics of wire ropes, International Journal of Fatigue 103 (2017) 456–465. doi:10.1016/j.ijfatigue.2017.06.024.

[5] R. Hobbs, K. Ghavani, The fatigue of structural wire strands, International Journal of Fatigue 4 (2) (1982) 69–72. doi:10.1016/0142-1123(82)90062-7.

[6] N. Casey, W. Lee, The fatigue failure of large diameter six strand wire rope, International Journal of Fatigue 11 (2) (1989) 78–84.

[7] D. Zhang, S. Ge, Y. Qiang, Research on the fatigue and fracture behavior due to the fretting wear of steel wire in hoisting rope, Wear 255 (7-12) (2003) 1233–1237. doi:10.1016/S0043-1648(03)00161-3.

[8] A. Cruzado, M. Hartelt, R. Wäsche, M. Urchegui, X. Gómez, Fretting wear of thin steel wires. Part 1: Influence of contact pressure, Wear 268 (11-12) (2010) 1409–1416. doi:10.1016/j.wear.2010.02.017.

[9] D. Wang, D. Zhang, S. Ge, Effect of displacement amplitude on fretting fatigue behavior of hoisting rope wires in low cycle fatigue, Tribology International 52 (2012) 178–189. doi:10.1016/j.triboint.2012.04.008.

[10] J. Winkler, C. T. Georgakis, G. Fischer, Fretting fatigue behavior of high-strength steel monostrands under bending load, International Journal of Fatigue 70 (2015) 13–23. doi:10.1016/j.ijfatigue.2014.08.009.

[11] I. Argatov, X. Gómez, W. Tato, M. Urchegui, Wear evolution in a stranded rope under cyclic bending: Implications to fatigue life estimation, Wear 271 (11-12) (2011) 2857–2867. doi:10.1016/j.wear.2011.05.045.

[12] D. Wang, D. Zhang, S. Wang, S. Ge, Finite element analysis of hoisting rope and fretting wear evolution and fatigue life estimation of steel wires, Engineering Failure Analysis 27 (2013) 173–193. doi:10.1016/j.engfailanal.2012.08.014.

[13] J. Toribio, Relationship between microstructure and strength in eutectoid steels, Materials Science and Engineering: A 387-389 (2004) 227–230. doi:10.1016/j.msea.2004.01.084.

[14] J. Toribio, A. Valiente, Failure analysis of cold drawn eutectoid steel wires for prestressed concrete, Engineering Failure Analysis 13 (3) (2006) 301–311. doi:10.1016/j.engfailanal.2005.03.003.

[15] M. Bonneric, V. Aubin, D. Durville, Finite element simulation of a steel cable - rubber composite under bending loading: Influence of rubber penetration on the stress distribution in wires, International Journal of Solids and Structures 160 (2019) 158–167. doi:10.1016/j.ijsolstr.2018.10.023.